

## Cyclic testing of steel column-tree moment connections with various beam splice lengths

Kangmin Lee<sup>1</sup>, Rui Li<sup>\*1</sup>, Liuyi Chen<sup>1</sup>, Keunyeong Oh<sup>1</sup> and Kang-Seok Kim<sup>2</sup>

<sup>1</sup> Department of Architectural Engineering, Chungnam National University,  
220 Gung-dong, Yuseong-gu, Daejeon, 305-764, Korea

<sup>2</sup> Facilities Operations Team, Daejeon-Chungnam District Division, Korea Electric Power CO,  
9-7 Yongjeon-dong, Dong-gu, Daejeon, 300-713, Korea

(Received July 02, 2013, Revised October 19, 2013, Accepted October 29, 2013)

**Abstract.** The purpose of this study was to evaluate the cyclic behavior of steel column-tree moment connections used in steel moment resisting frames. These connections are composed of shop-welded stub beam-to-column connection and field bolted beam-to-beam splice. In this study, the effects of beam splice length on the seismic performance of column-tree connections were experimentally investigated. The change of the beam splice location alters the bending moment and shear force at the splice, and this may affect the seismic performance of column-tree connections. Three full-scale test specimens of column-tree connections with the splice lengths of 900 mm, 1,100 mm, and 1,300 mm were fabricated and tested. The splice lengths were roughly 1/6, 1/7, 1/8 of the beam span length of 7,500 mm, respectively. The test results showed that all the specimens successfully developed ductile behavior without brittle fracture until 5% radians story drift angle. The maximum moment resisting capacity of the specimens showed little differences. The specimen with the splice length of 1,300 mm showed better bolt slip resistance than the other specimens due to the smallest bending moment at the beam splice.

**Keywords:** column-tree connection; moment resisting frame; cyclic testing; seismic performance; bolt slip

---

### 1. Introduction

Construction using moment resisting frames is considered one of the most reliable earthquake resistance systems. This confidence was greatly shaken after the 1994 Northridge earthquake since many steel moment resisting frames suffered damage. Brittle fractures occurred at the beam-to-column joint, resulting from several factors, such as stress concentration in weld access hole regions, crack initiation due to back-up bars at the beam bottom flanges and weld defects (Mahin 1998 and Miller 1998). Hence, various studies on the seismic performance of beam-to-column moment connections have been conducted. Prequalified connections were developed through research on the seismic performance of beam-to-column connections (FEMA 2000) in the US. These post-Northridge connections include reduced beam section connections (Jones *et al.* 2002 and Tabar and Deylami 2006), reinforced connections (Kim *et al.* 2002 and Chou *et al.* 2010), and

---

\*Corresponding author, Graduate Student, E-mail: [lirui@cnu.ac.kr](mailto:lirui@cnu.ac.kr)

semi-rigid connections (Girão Coelho and Bijlaard 2007, Drosopoulos *et al.* 2012, and Valipour and Bradford 2013).

The column-tree connection is one of the beam-to-column connections frequently used in moment resisting frames in Korea and Japan. The column-tree connection is fabricated by welding a stub beam (generally 600 to 1,200 mm long) to a column in the shop. Then a mid-portion of the beam is spliced to the stub beam after the shop fabricated column-tree is erected in the field. There are various options for the splice joining the inner span beam to the column-tree. The splice of the column-tree assembly to an inner beam can be fully bolted, welded and bolted, or fully welded (Astaneh-Asl 1997). Chen *et al.* (2006) carried out analytical and experimental studies on the cyclic behavior of widened flange column-tree connections. The widened flange connection associated with no weld access hole detail could diminish the potential for brittle fracture caused by the peak plastic strain demand in the weld access hole region as experienced in the pre-Northridge connection details. Six column-tree connections proposed by widening and tapering the portion of beam flanges to increase the ductility and strength of the connection were tested (Chen and Lin 2013). All of the proposed tapered beam flange specimens achieved satisfactory ductile behavior by forming a plastic hinge in the beam section away from the column face. McMullin and Astaneh-Asl (2003) carried out analytical studies of semi-rigid column-tree connections for the global performance of structures, and this study showed that global performance was enhanced for a 4-story building and a 24-story building by switching from rigid to semi-rigid frame construction.

For column-tree connections, one of the key design issues is the beam splice length. Changing the beam splice location could alter the bending moment and shear force at the beam splice, and this may affect the seismic performance. In general, the beam splice should be placed at the inflection point of the beam under gravity load only conditions. However, the actual force distribution under seismic loading is more complex, so it is difficult for the designer to specify the minimum strength requirement at the beam splice. Therefore, the cyclic testing of three full-scale column-tree connection specimens was conducted to verify the effects of the beam splice location.

## 2. Experimental programs

Three full-scale test specimens of column-tree connections, designed and detailed according to the AISC Seismic Provisions (AISC 2010), were fabricated and tested. Quasi-static cyclic loading was applied to the specimens to investigate the cyclic behavior of column-tree connections. As mentioned earlier, the test variable was the location of the beam splice.

### 2.1 Test specimens

The first step in the design of a column-tree connection is to decide the location of the beam splice. The beam splice can be placed at the beam inflection point under gravity load only. Since this inflection point can migrate under service loading and actual forces and moments may differ significantly from those assumed, it is prudent for the designer to specify the minimum strength requirement at the splice. Astaneh-Asl (1997) proposed that beam splices in fixed-ended beams be located at a distance of  $l/8$  to  $l/6$  from the centerline of the column, where  $l$  is the span length of the beam. In addition, with current transportation limitations, it is suggested that the splices be placed such that the total length of the column trees does not exceed 2,500 mm. On the other hand,

if the location of the beam splice is too close to the column face, it prevents the development of the plastic hinge at the end of the beam.

In this study, three specimens with different splice lengths were designed. The beam splice location of specimen CTD01 was at a distance of 900 mm from the column face, which was about 1/7 of the beam span length; that of specimen CTD 02 was at a distance of 700 mm from the column face, which was about 1/6 of the beam span length; and that of specimen CTD03 was at a distance of 1100 mm from the column face, which was about 1/8 of the beam span length. Welded unreinforced flange – welded web (WUF-W) connections (Han S W *et al.* 2007 and Roeder C W 2002) were used for the beam-column joint of all specimens. These connections utilized complete joint penetration (CJP) groove welds to join beam flanges to column flanges. Web joints were made with CJP groove welds of the beam web to the column flange.

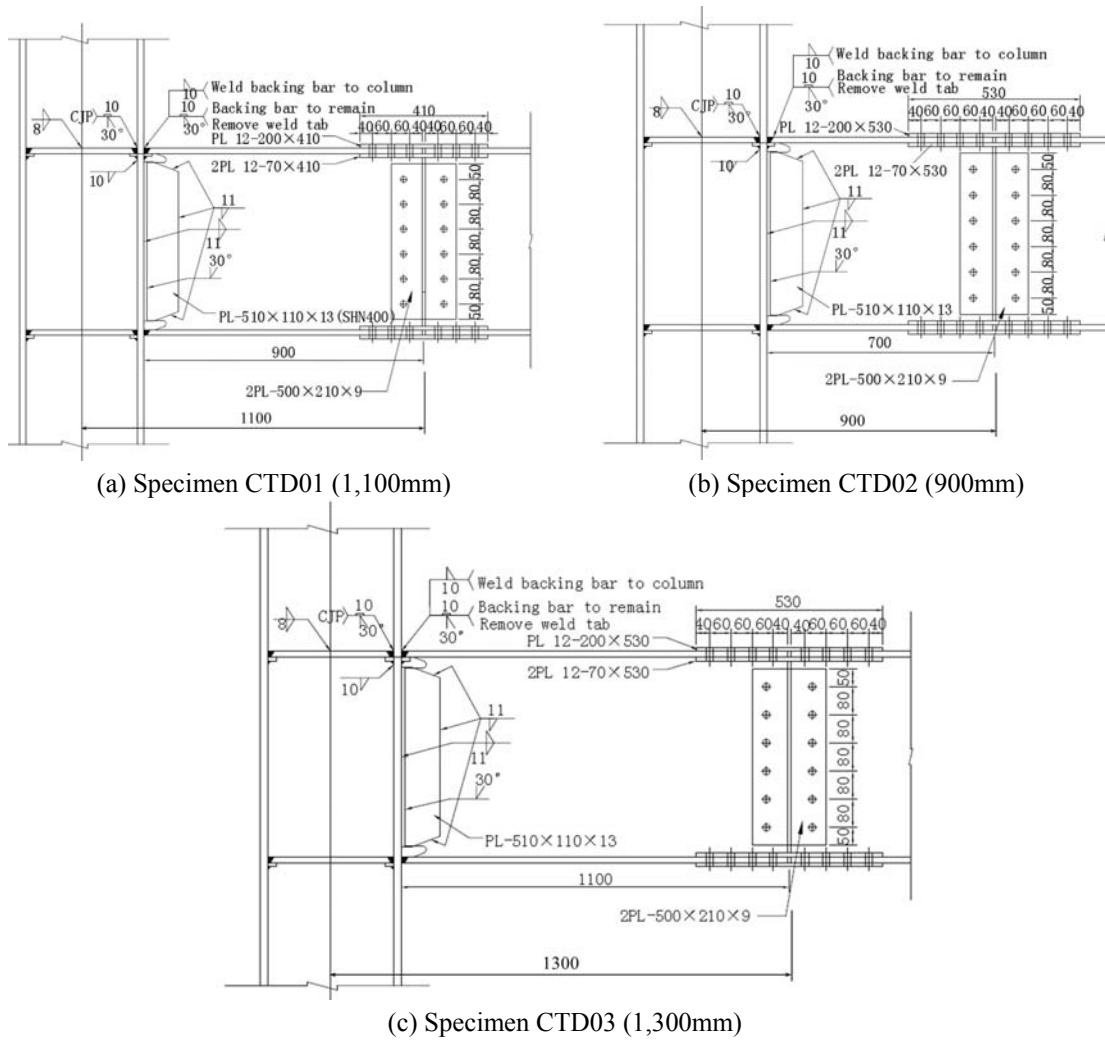


Fig. 1 Details of the specimens

Table 1 Column-tree connection specimens

Specimen	Location of beam splice(mm)	Flange splice			Web splice	
			Flange plates	Bolts	Web plates	Bolts
CTD01	1,100	Top	PL 12-200 × 530	32	PL 9-210 × 500	12
		Bottom	2PL 12-70 × 530			
CTD02	900	Top	PL 12-200 × 530	32	PL 9-210 × 500	12
		Bottom	2PL 12-70 × 530			
CTD03	1,300	Top	PL 12-200 × 530	32	PL 9-210 × 500	12
		Bottom	2PL 12-70 × 530			

The specimens were fabricated using standard rolled H-shaped steel. All specimens comprised H-600 × 200 × 11 × 17 beams and H-400 × 400 × 13 × 21 columns. High-strength bolts of  $\Phi$ -20 ( $F_u = 1,000$  MPa) were used to splice the beams. The notch-tough welding materials, improved welding procedures, and modified access hole geometry specified in the AISC Seismic Provisions were used for all specimens. The size and details of the specimens are shown in Fig. 1. Table 1 summarizes the properties of each specimen.

Each specimen was designed to satisfy the panel zone strength requirements in the AISC seismic provisions. To prevent soft-story damage, the strong column-weak beam criteria is satisfied by having the ratio of the sum of the column nominal flexural capacity to the sum of the beam expected flexural capacity equal to a value greater than 1.0 for each specimen, where and are the capacities extrapolated to the intersection of the beam and column centerlines in accordance with the AISC seismic provisions.

## 2.2 Material properties

The beams and columns for all specimens were fabricated with SHN400 steel (nominal yield strength, = 235 MPa and nominal tensile strength, = 400 MPa) and SHN490 steel (= 325 MPa and = 490 MPa), respectively. The mechanical properties of the steel sections are given in Table 2. These properties were obtained from testing of standard tensile coupons. The coupon test results are also summarized in Table 2.

Table 2 Coupon test results

Shape	Location	Steel	$F_y$ (MPa)	$F_u$ (MPa)	$F_{ye}$ (MPa)	$F_{ue}$ (MPa)
H-400 × 400 × 13 × 21 (Column)	Web	SHN490	325	490	398.4	559.7
	Flange	SHN490	325	490	407.9	571.4
H-600 × 200 × 11 × 17 (Beam)	Web	SHN400	235	400	336.3	470.5
	Flange	SHN400	235	400	292.3	455.8

2.3 Test setup, loading protocol and instrumentation

Fig. 2 shows a schematic view of the test set-up. As shown in the figure, the column of specimen was fixed to the floor, and the free end of the beam was connected to the actuator for cyclic loading. Lateral supports were provided to prevent out-of-plane instability and twisting of the beam.

The specimens were tested by application of a prescribed quasi-static cyclic story drift history based on the loading protocol defined in Section S6.2 of the AISC seismic provisions. A 500 kN capacity actuator was used to impose the predetermined cyclic loads. The loading protocol comprised six cycles each of 0.375, 0.5, and 0.75% story drift ratio, followed by four cycles of 1.0% story drift ratio and two cycles each of 1.5, 2, 3, 4 and 5% story drift ratio. A test was terminated when either a fracture occurred, resulting in a significant loss of specimen capacity, or after a story drift ratio of 5% was reached, which was the maximum drift the test setup could accommodate. The loading sequence is shown in Fig. 3.

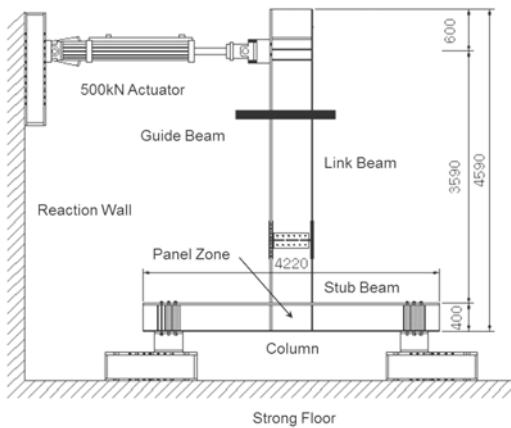


Fig. 2 Test setup

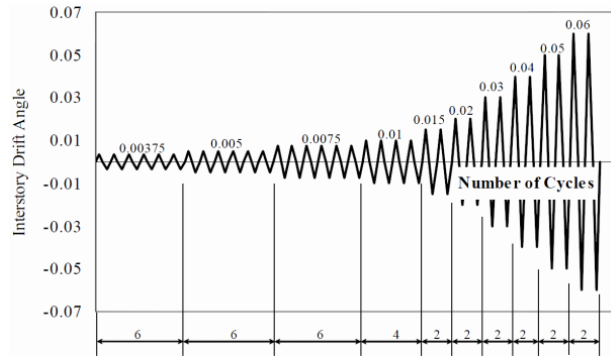


Fig. 3 Loading protocol

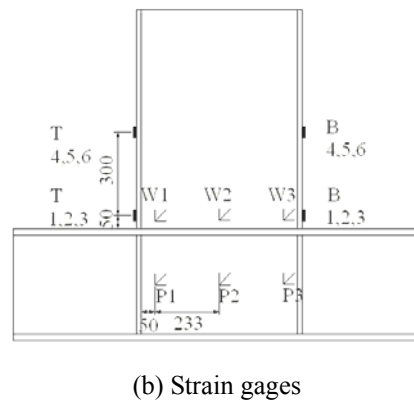
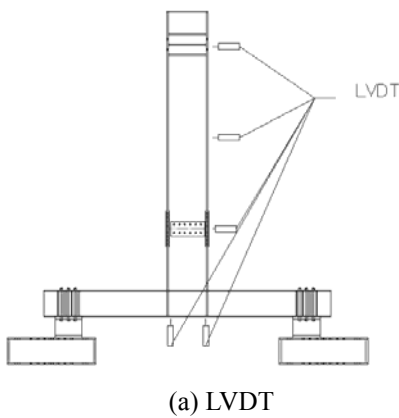


Fig. 4 Gage Layouts

Linear varying displacement transducers (LVDTs) were attached to the specimens to measure the displacement of structures. The maximum stroke of a  $\pm 300$  mm LVDT was used at the tip of the beam. Two LVDTs with  $\pm 100$  mm capacity were installed at the location of the beam splice and the mid-span of the beam, respectively. Two LVDTs with  $\pm 50$  mm capacity were installed inside of the panel zone to measure the deformation of the panel zone. Strain gauges were attached to the beam flanges, flange plates, and beam webs along the depth of the shear tab and the panel zone. The layout of the LVDTs and the arrangement of the strain gages are presented in Fig. 4. Before testing, the specimens were whitewashed to observe the yielding of the components during the tests.

### 3. Test results

The relationship of the beam normalized moment at the column face to the story drift of specimens are shown in Fig. 5, where  $\mu$  is the story drift ratio,  $M_c$  is the beam moment at the column face obtained from the test results, and  $M_p$  is the beam plastic moment capacity. As seen in Fig. 5, the beam maximum moment of each specimen is about 1.5 times higher than the beam plastic moment. For all three specimens, their maximum bending moment resistances were very similar. This indicates that the location of the beam splice does not affect the maximum moment resisting capacity of column-tree connections. A summary of the response of each specimen is given in Table 3, including the maximum horizontal load at the end of the beam; the slip resistance at the splice; the maximum beam normalized moment at the column face; the maximum story drift ratio; the total plastic rotation; the maximum plastic rotation developed in the panel zone, beam, stub beams, and link beam.

The following discusses detailed experimental observations during the testing of three column-tree moment connection specimens.

#### 3.1 Specimen CTD01

The beam splice location of specimen CTD01 was at a distance of 900 mm from the column face. During the cycles of 1% story drift ratio, the bolt slip at the beam splice of the specimen was observed as shown in Fig. 6(a). The slip load was 95 kN. Yielding of the beam flanges was detected during the cycles of 1.5% story drift ratio. Then, yielding occurred in the corners of the column panel zone, followed by the beam flange, as shown in Fig. 6(b). At the cycles of 3% story drift ratio, stress concentration at the access hole was clearly observed. During the cycles of 4% story drift ratio, a crack at the end of the access hole near the beam web CJP groove weld was detected. Then, local buckling of the beam flanges occurred at the cycles of 5% story drift ratio as shown in Fig. 6(c). The maximum magnitude of load before local buckling was 282 kN. After the cycles of 5% story drift ratio were completed, the specimen was pushed to its ultimate capacity, and the test was stopped because of the actuator stroke limit.

#### 3.2 Specimen CTD02

The beam splice location of specimen CTD02 was at a distance of 700 mm from the column face. During the cycles of 0.75% story drift ratio, bolt slip was detected at the beam splice. The slip load was 75 kN. The bolt slip of specimen CTD02 occurred earlier than that of specimen CTD01. This result was expected since the moment of specimen CTD02 at the beam splice was

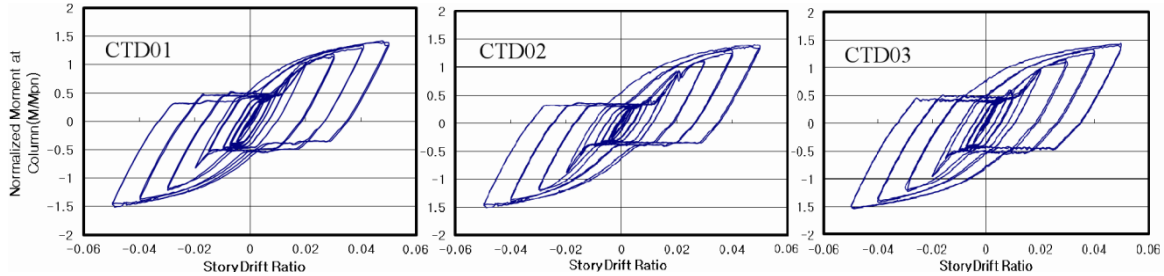


Fig. 5 Hysteretic curves of story drift ratio

Table 3 Summary of test results

Specimen	CTD01	CTD02	CTD03
Max. resistance strength (kN), $P_u$	282	287	286
Slip resistance strength (kN), $P_s$	95	75	105
Max. normalized moment, $M_f/M_p$	1.51	1.54	1.53
Max. story drift (rad), $\delta_t$	0.0497	0.0496	0.0497
Total plastic rotation (rad), $\theta_t$	0.0416	0.0415	0.0416
Beam plastic rotation (rad), $\theta_b$	0.0226	0.0224	0.0209
Stub beam plastic rotation (rad), $\theta_{sb}$	0.0121	0.0096	0.0137
Link beam plastic rotation (rad), $\theta_{lb}$	0.0105	0.0138	0.0072
Panel zone plastic rotation (rad), $\theta_{pz}$	0.0190	0.0181	0.0199



(a) Bolt slip



(b) Yielding of panel zone



(c) Flange buckling

Fig. 6 Photographs of specimen CTD01 during testing

greater than that of specimen CTD01. The yielding of the beam flanges occurred during the cycles of 2% story drift ratio. Yielding occurred in the corners of the column panel zone, followed by the beam flange. At the cycles of 4% story drift ratio, yielding occurred in the column flange. Then, local buckling of the beam flanges occurred at the cycles of 5% story drift ratio. Also, a tiny crack appeared at the weld joint of the beam flange and the column flange. The maximum magnitude of

load before local buckling was 287 Kn.

### 3.3 Specimen CTD03

The beam splice location of specimen CTD03 was at a distance of 1,100 mm from the column face. During the cycles of 1% story drift ratio, bolt slip was detected at the beam splice. The slip load was 105 kN. The slip load of specimen CTD03 was higher than that of specimen CTD01. During the cycles of 1.5% story drift ratio, the yielding of beam flanges occurred. At the cycles of 2% story drift ratio, stress concentration at the access hole was also observed. At the cycles of 3% story drift ratio, the entire panel zone yielded. At the cycles of 4% story drift ratio, yielding in the beam web was clearly observed. Then, local buckling of the beam flanges occurred. The maximum magnitude of load before local buckling was 286.9 kN.

## 4. Analysis of test result and investigation

### 4.1 Strain distributions

The strain distribution across the width of the beam bottom flange near the column face at 4% and 5% story drift are shown in Figs. 7 and 8, respectively, for the all test specimens. At 4% story drift, specimens CTD02 and CTD03, having developed significant local beam flange buckling, showed a strain gradient across the beam compression flange with a significant portion of the flange yielding. The strain distribution for specimen CTD01 was more uniform than that for the other specimens. At 5% story drift, specimen CTD01 also developed significant local beam flange buckling. The strain at the middle of the flange plate located in the beam splice for 4% and 5% story drift is shown in Fig. 9 for the all test specimens. The strain of specimen CTD 02 at the middle of the flange plate was the highest among all specimens because the moment of specimen CTD02 at the beam splice was greater than that of the other two specimens. The strain of specimen CTD01 and CTD02 clearly increased at 5% story drift; however, that of specimen CTD03 remained unchanged.

### 4.2 Deformation capacity

According to the requirement of Seismic Provisions for Structural Steel Buildings,

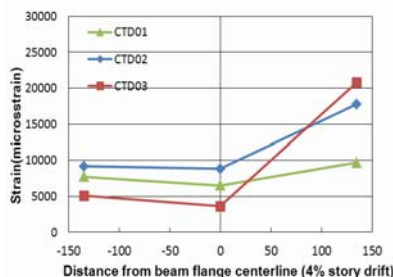


Fig. 7 Beam flange strain distribution at 4% story drift

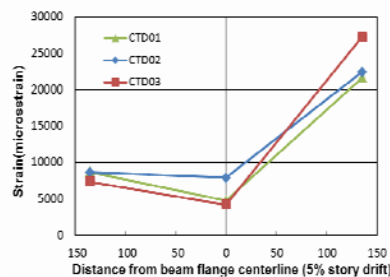


Fig. 8 Beam flange strain distribution at 5% story drift

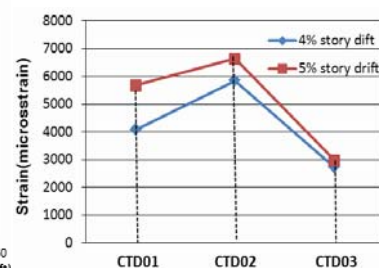


Fig. 9 Strain at the middle of the flange plate

beam-to-column connections used in special moment frames (SMF) must be capable of sustaining a story drift ratio of at least 0.04 radians. All specimens showed the best seismic performance such that the maximum story drift ratio reached 0.05 radians. The test results indicate that column-tree connections are qualified for SMF.

A summary of the contribution of the stub beam, link beam, and panel zone to the total inelastic rotation for each specimen at 5% story drift is given in Fig. 10. Because the design of each specimen followed the weak beam-strong column concept, the column deformation is very slight in general. Thus, the contributions of the column to the story drift could be ignored.

The majority of the inelastic rotation was contributed by the beams. The contribution of the panel zone of specimens CTD01, CTD02 and CTD03 to the total inelastic rotation at 5% story drift was 46.7%, 43.6%, and 47.8% of , while the beams contributed 53.3%, 56.4%, and 52.2% of . The contribution of the stub beam of specimens CTD01, CTD02 and CTD03 to the beam inelastic rotation at 5% story drift was 53.5%, 42.9%, and 65.5% of . The stub beam contribution to the total plastic rotation was related to the length of the stub beam. The contribution of the stub beam increased when the length of the stub beam increased, as shown in Fig. 10. This is inevitable because the deformation of the longer beam must be greater. The contribution of the panel zone to the total plastic rotation also increased when the length of the stub beam increased. If the plastic rotation of the panel zone is greater, the plastic rotation of the beam will be smaller when the total plastic rotation is a constant value. The strain in the end of the beam could be reduced due to the reduced beam deformation; thus, it may reduce the risk of fracture of the beam flange.

### 4.3 Energy dissipation

Energy dissipation capacity is an important index to evaluate the seismic performance of beam-to-column moment connections, and it can be reflected through the area of the load-displacement hysteretic loop. A summary of the accumulated energy dissipation of each specimen is shown in Fig. 11. Among the three column-tree connection specimens, specimen CTD03 dissipated the largest amount of energy, while specimen CTD02 dissipated the lowest amount of energy. This indicates that when the location of the beam splice was farther from the column face, the energy dissipation capacity of column-tree connections was higher.

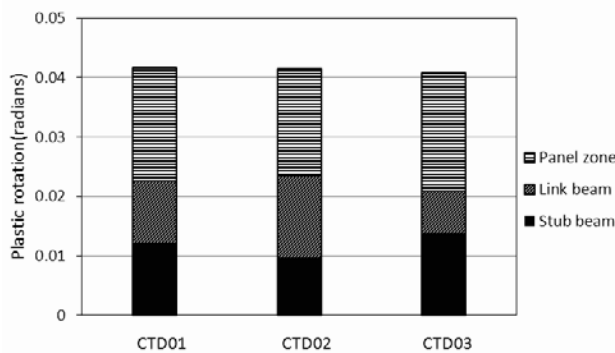


Fig. 10 Summary of specimen plastic rotation components

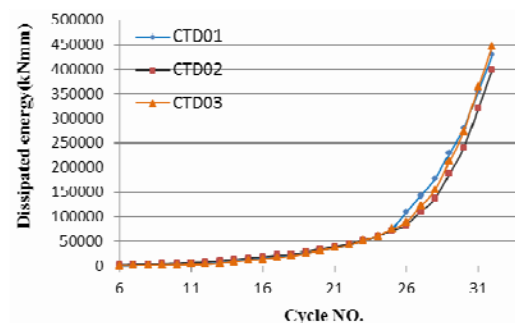


Fig. 11 Comparison of accumulated energy dissipation

## 5. Conclusions

Three full-scale column-tree connection specimens were tested to investigate their seismic performance. The following conclusions can be drawn from the experimental study:

- (1) The column-tree connection specimens successfully achieved a 5% radians story drift ratio without brittle fracture. The failure mode of these specimens was the local buckling of the beam flanges. The specimens met the qualification criteria required by the AISC Seismic Provisions (AISC 2010) for use in SMFs.
- (2) The maximum bending moment resistance of the three specimens was very similar. This indicates that the location of the beam splice does not affect the maximum bending moment resistance of column-tree connections. However, the slip load of each specimen was different. Specimen CTD03 showed higher bolt slip resistance than the other specimens because the bending moment of specimen CTD03 at the beam splice was the smallest.
- (3) The energy dissipation capacity of the column-tree connection specimens increased with longer beam splices. The stub beam contribution to the total plastic rotation was also related to the length of the stub beam.

## Acknowledgments

This research was supported by Basic Science Research Program through the National Research Foundation of Korea (NRF) funded by the Ministry of Education, Science and Technology (grant number: 2012R1A1A4A01004350).

## References

- AISC (2010), *Seismic Provision for Structural Steel Building*, American Institute of Steel Structure, Chicago, IL, USA.
- Astaneh-Asl, A. (1997), "Seismic design of steel column-tree moment-resisting frames", *Struct. Steel Edu. Council*.
- Chen, C.C., Lin, C.C. and Lin, C.H. (2006), "Ductile moment connections used in steel column-tree moment-resisting frames", *J. Construct. Steel Res.*, **62**(8), 793-801.
- Chen, C.C. and Lin, C.C. (2013), "Seismic performance of steel beam-to-column moment connections with tapered beam flanges", *Eng. Struct.*, **48**, 588-601.
- Chou, C.C., Tsai, K.C., Wang, Y.Y. and Jao, C.K. (2010), "Seismic rehabilitation performance of steel side plate moment connections", *Earthq. Eng. Struct. Dyn.*, **39**(1), 23-44.
- Drosopoulos, G.A., Stavroulakis, G.E. and Abdalla, K.M. (2012), "3D Finite element analysis of end-plate steel joints", *Steel Compos. Struct., Int. J.*, **12**(2), 93-115.
- FEMA (2000), *Recommended Seismic Design Criteria for New Steel Moment-Frame Buildings: FEMA-350*, SAC Joint Venture, Richmond, CA, USA.
- Girão Coelho, A.M. and Bijlaard, F.S.K. (2007), "Experimental behavior of high strength steel end-plate connections", *J. Construct. Steel Res.*, **63**(9), 1228-1240.
- Han, S.W., Kwon, G.U. and Moon, K.H. (2007), "Cyclic behaviour of post-Northridge WUF-B connections", *J. Construct. Steel Res.*, **63**(3), 365-374.
- Jones, S.L, Fry, G.T. and Engelhardt, M.D. (2002), "Experimental evaluation of cyclically loaded reduced beam section moment connections", *J. Struct. Eng.*, **128**(4), 441-451.
- Kim, T., Whittaker, A.S., Gilani, A.S.J., Bertero, V. and Takhirov, S. (2002), "Experimental evaluation of

- plate-reinforced steel moment-resisting connections”, *J. Struct. Eng.*, **128**(4), 483-491.
- Mahin, S.T. (1998), “Lessons from damage to steel buildings during the Northridge earthquake”, *Eng. Struct.*, **20**(4-6), 261-270.
- McMullin, K.M. and Astaneh-Asl, A. (2003), “Steel semirigid column-tree moment resisting frame seismic behavior”, *J. Struct. Eng.*, **129**(9), 1243-1249.
- Miller, D.K. (1998), “Lessons learned from the Northridge earthquake”, *Eng. Struct.*, **20**(4-6), 249-260.
- Roeder, C.W. (2002), “Connection performance for seismic design of steel moment frames”, *J. Struct. Eng.*, **128**(4), 517-525.
- Tabar, A.M. and Deylami, A. (2006), “Investigation of major parameters affecting instability of steel beams with RBS moment connections”, *Steel Compos. Struct., Int. J.*, **6**(3), 203-219.
- Valipour, H.R. and Bradford, M.A. (2013), “Nonlinear P- $\Delta$  analysis of steel frames with semi-rigid connections”, *Steel Compos. Struct., Int. J.*, **14**(1), 1-20.

CC